Journal of General Virology (2010), **91**, 2019–2028 DOI 10.1099/vir.0.019257-0

Replication kinetics of neurovirulent versus non-neurovirulent equine herpesvirus type 1 strains in equine nasal mucosal explants

Annelies P. Vandekerckhove,[1] S. Glorieux,[1] A. C. Gryspeerdt,[1] L. Steukers,[1] L. Duchateau,[2] N. Osterrieder,[3] G. R. Van de Walle[1,2]† and H. J. Nauwynck[1]†

Correspondence
G. R. Van de Walle
gerlinde.vandewalle@UGent.be

[1]Department of Virology, Parasitology and Immunology, Faculty of Veterinary Medicine, Ghent University, Salisburylaan 133, B-9820 Merelbeke, Belgium

[2]Department of Physiology and Biometrics, Faculty of Veterinary Medicine, Ghent University, Salisburylaan 133, B-9820 Merelbeke, Belgium

[3]Institut für Virologie, Freie Universitaet Berlin, Philippstrasse 13, 10115 Berlin, Germany

Equine herpesvirus type 1 (EHV-1) is the causative agent of equine herpes myeloencephalopathy, of which outbreaks are reported with increasing frequency throughout North America and Europe. This has resulted in its classification as a potentially emerging disease by the US Department of Agriculture. Recently, it was found that a single nucleotide polymorphism (SNP) in the viral DNA polymerase gene (ORF30) at aa 752 (N→D) is associated with the neurovirulent potential of EHV-1. In the present study, equine respiratory mucosal explants were inoculated with several Belgian isolates typed in their ORF30 as D_{752} or N_{752}, to evaluate a possible difference in replication in the upper respiratory tract. In addition, to evaluate whether any observed differences could be attributed to the SNP associated with neurovirulence, the experiments were repeated with parental Ab4 (reference neurovirulent strain), parental NY03 (reference non-neurovirulent strain) and their N/D revertant recombinant viruses. The salient findings were that EHV-1 spreads plaquewise in the epithelium, but plaques never cross the basement membrane (BM). However, single EHV-1-infected cells could be observed below the BM at 36 h post-inoculation (p.i.) for all N_{752} isolates and at 24 h p.i. for all D_{752} isolates, and were identified as monocytic cells and T lymphocytes. Interestingly, the number of infected cells was two to five times higher for D_{752} isolates compared with N_{752} isolates at every time point analysed. Finally, this study showed that equine respiratory explants are a valuable and reproducible model to study EHV-1 neurovirulence *in vitro*, thereby reducing the need for horses as experimental animals.

Received 18 December 2009
Accepted 25 April 2010

INTRODUCTION

Equine herpesvirus 1 (EHV-1) is a ubiquitous respiratory viral pathogen that causes serious economic losses in the horse industry worldwide (Allen & Bryans, 1986; Bryans & Allen, 1989; Brosnahan & Osterrieder, 2009). EHV-1 exerts its impact by causing respiratory tract disease, but it can also cause abortion, neonatal foal death and nervous system disorders (Patel & Heldens, 2005; Lunn *et al.*, 2009). The mucosa of the upper airway tract is the first line of defence against respiratory diseases (Timoney, 2004). It is also the primary replication site of EHV-1, as it is for most alphaherpesviruses (Kydd *et al.*, 1994a; Van Maanen, 2002; Van Maanen & Cullinane, 2002; Gryspeerdt *et al.*, 2010). Subsequently, the virus disseminates via a leukocyte-associated viraemia, which enables EHV-1 to reach end-vessel endothelia in the uterus and central nervous system (Allen & Bryans, 1986; Kydd *et al.*, 1994b). In these organ systems, virus replication can result in vasculitis and perivasculitis, ultimately resulting in abortion and myeloencephalopathy, respectively. Devastating outbreaks of equine herpes myeloencephalopathy are reported with increasing frequency throughout North America and Europe (Kohn *et al.*, 2006; Perkins *et al.*, 2009; Pusterla *et al.*, 2009), resulting in its classification as a potentially emerging disease by the US Department of Agriculture's Animal and Plant Health Inspection Service (USDA APHIS, 2007).

Recently, it was shown by Nugent *et al.* (2006) that a single nucleotide polymorphism (SNP) in the catalytic subunit of the viral DNA polymerase, encoded by open reading frame

†These authors contributed equally to this work.

(ORF) 30, causing a substitution of asparagine (N) by aspartic acid (D) at aa 752, is significantly associated with the neurovirulent potential of naturally occurring strains. The causal relationship between this SNP in EHV-1 polymerase and neuropathogenicity in the horse was further confirmed through targeted mutagenesis of this single nucleotide in the genome of EHV (Goodman *et al.*, 2007; Van de Walle *et al.*, 2009). Unfortunately, to date, studies to compare neurovirulent and non-neurovirulent EHV-1 isolates can only be carried out in its natural host, the horse. The murine model of EHV-1 infection is a valuable model to study EHV-1 *in vivo* (Awan *et al.*, 1990; Van Woensel *et al.*, 1995; Galosi *et al.*, 2004); however, it cannot be used to study EHV-1 neuropathogenicity (Goodman *et al.*, 2007). To compare the growth kinetics of neurovirulent and non-neurovirulent EHV-1 strains, an *in vitro* model of mouse cerebral cortex cells has been described, but no convincing correlation between the D/N difference in ORF30 and replication efficiency in murine neurons has been observed (Yamada *et al.*, 2008). Consequently, there is a huge need for alternative models to study EHV-1 neuropathogenicity to minimize the necessity of using horses as experimental animals. Previously, we successfully established an *in vitro* model of equine respiratory mucosal explants (Vandekerckhove *et al.*, 2009). Such explant models provide accessible means to mimic the *in vivo* situation, as three-dimensional structure and normal cell–cell contacts are maintained (Glorieux *et al.*, 2007; Vandekerckhove *et al.*, 2009). Hence, *in vitro* equine respiratory mucosal explants might provide not only a good alternative to reduce the number of *in vivo* horse experiments, but also a useful tool to obtain more detailed information on the invasion mechanisms of EHV-1 in general and specifically the difference between neurovirulent and non-neurovirulent isolates.

Therefore, the aim of the present study was to unravel the invasion mechanisms and kinetics of EHV-1 in the equine respiratory mucosal explant model. In addition, several non-neurovirulent (N_{752}) and neurovirulent (D_{752}) EHV-1 isolates were tested in this explant model to evaluate its potential to discriminate between isolates, evaluate their effect on leukocytes and ultimately contribute to an improved characterization of the pathogenesis of EHV-1 neurological disease.

RESULTS

Evaluation of EHV-1 replication in equine respiratory nasal mucosal explants

Nasal and nasopharyngeal explants of three individual horses were inoculated with the D_{752} isolate 03P37, whilst nasal and nasopharyngeal explants of three other horses were inoculated with the N_{752} isolate 97P70. For each animal, one explant was examined at each collected time point [0, 12, 24, 36, 48 and 72 h post-inoculation (p.i.)].

For both isolates, single infected cells in the epithelium were visible at 12 h p.i., which mainly consisted of epithelial cells, with a rare infected macrophage or $CD5^+$ T lymphocyte (data not shown). For both strains, EHV-1-induced epithelial plaques were observed from 24 h p.i. onwards, which increased in both volume and latitude over time, with a significant increase between 36 and 48 h p.i. ($P<0.0001$ for both 03P37 and 97P70, Fig. 1a, b). At 48 and 72 h p.i., a significant difference in plaque volume was observed between 03P37 and 97P70 (Fig. 1b). In addition, the number of plaques also increased over time, especially between 36 and 48 h p.i., but without any significant difference between the strains (Fig. 1d). Interestingly, EHV-1-induced plaques did not cross the basement membrane (BM) at any observed time point p.i., but individual EHV-1-infected cells in the connective tissue were observed below the BM (Fig. 1c). Here, a difference between these two strains was observed when evaluating the time point of BM crossing of the basement membrane via single EHV-1-infected cells. For 97P70, a non-neurovirulent (N_{752}) isolate, individual infected cells were present below the BM starting from 36 h p.i. (Fig. 2b). EHV-1-infected cells were present in all examined regions for both nasal septum and nasopharynx, but were mainly situated below EHV-1-induced plaques in the epithelium (Fig. 2a, b, regions A and B) and their number increased over time (Fig. 2b). In contrast, for 03P37, a neurovirulent (D_{752}) EHV-1 isolate, individual infected cells below the BM were already present at 24 h p.i. (Fig. 2b). These results indicated a difference between the strains regarding the moment when they are able to cross the BM barrier via single EHV-1-infected cells, and could suggest a difference in invasion kinetics between neurovirulent and non-neurovirulent strains. Furthermore, a difference in leukocyte tropism was also observed between both strains. For 97P70, the N_{752} strain, individual infected cells were equally identified as $CD5^+$ T lymphocytes and $CD172a^+$ monocytic cells (Table 1). B cells were present, but were rarely infected (Table 1). EHV-1-infected $CD5^+$ T lymphocytes were further characterized and consisted mainly of $CD4^+$ T lymphocytes, but $CD8^+$ T lymphocytes were also susceptible to infection (Table 1). For 03P37, the D_{752} strain, however, the majority of individual infected cells were $CD172a^+$, and only a small portion of EHV-1 carrier cells were identified as $CD5^+$ T lymphocytes (Table 1). Here also, both T-lymphocyte subpopulations were equally infected with EHV-1, and B lymphocytes were rarely infected (Table 1).

In conclusion, this experiment indicated a difference in (i) invasion kinetics (time point of crossing the BM barrier via single EHV-1-infected cells) and (ii) in cell tropism of the infected cells, between 97P70 and 03P37. However, as different horses were used for the inoculation with the two Belgian isolates, an influence of the donor horse and/or virus strains on the outcome of the experiment could not yet be excluded.

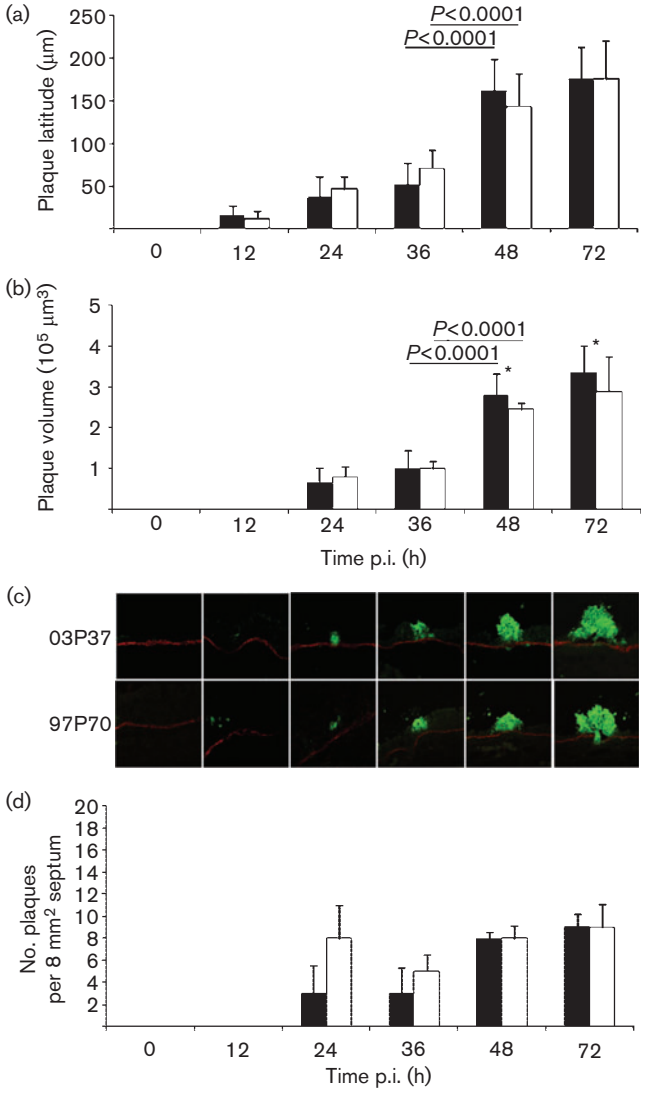

Fig. 1. Evolution of plaque formation in the epithelium of nasal septum explants. Equine respiratory mucosal explants were inoculated with the Belgian isolate 97P70 (N_{752}; empty bars) or 03P37 (D_{752}; filled bars). As results were identical upon infection of tissue from nasal septum or from nasopharynx, only data from the nasal septum are shown. At 0, 12, 24, 36, 48 and 72 h p.i., explants were collected and analysed. One hundred consecutive sections were prepared and several parameters were determined. All data shown represent means+SD of triplicate independent experiments, and *P* values for statistical significance are given for each strain. Asterisks indicate statistically significant differences ($P \leqslant 0.05$). (a, b) Plaque latitudes (a) and volumes (b) were measured for ten plaques at every time point and for each horse. (c) Representative confocal photomicrographs illustrating the evolution over time of EHV-1-induced plaques in the nasal septum (magnification ×20). (d) The number of plaques was determined at 0, 12, 24, 36, 48 and 72 h p.i. For each horse and isolate, 100 cryosections were analysed at every time point to count plaques.

Quantification of epithelial plaques and single EHV-1-infected cells of different Belgian EHV-1 isolates in respiratory nasal mucosal explants derived from the same horse

To substantiate our findings, identical experiments were performed with more Belgian D_{752} and N_{752} isolates, and this time all strains were inoculated on explants derived from the same horse to exclude any inter-horse variability.

In line with what was observed in the first experiment, no significant differences were observed in plaque latitude between the Belgian D_{752} and N_{752} isolates (Fig. 3a). A significant increase was also observed in plaque latitude from 24 to 48 h p.i. for all isolates ($P \leqslant 0.05$, Fig. 3a), with the exception of the D_{752} isolate 99P136, where only a slight increase was observed. For the number of plaques, no significant differences were observed between the isolates at 24 h p.i. (Fig. 3b). However, at 48 h p.i., significantly more plaques were observed for the isolates 94P247 and 97P70 carrying the N_{752} SNP compared with the D_{752} isolates ($P \leqslant 0.05$, Fig. 3b). This was in contrast to the first experiment, where no significant differences in number of plaques were observed between the D_{752} isolate 03P37 and the N_{752} isolate 97P70 at 48 h p.i. An explanation for this discrepancy in results could be that, in the second experiments, these isolates were tested on explants from the same horse, in contrast to the first experiment where different horses were used to evaluate the two isolates 03P37 and 97P70.

In the first experiment, a difference in invasion kinetics was observed between these two isolates and similar results were obtained in our second experiment. At 24 h p.i., single infected cells were present in the connective tissue below the BM barrier for all neurovirulent (D_{752}) isolates, in striking contrast to the non-neurovirulent N_{752} isolates where infection remained limited to the epithelium at that time point (Table 2). The vast majority of D_{752}-infected cells belonged to the $CD172a^+$ monocyte lineage (CML) and some cells were identified as $CD5^+$ T lymphocytes at that time point (Table 2). Also, isolate 03P37 infected twice as many immune cells in the lamina propria compared with all other D_{752} isolates (data not shown). At 48 h p.i., single EHV-1-infected cells were present in the lamina propria below the BM barrier for all EHV-1 isolates, irrespective of their genotype (Table 2). In general, individual infected cells were equally identified as $CD5^+$ T lymphocytes and $CD172a^+$ CML, irrespective of the D/N genotype (Table 2). The EHV-1-infected $CD5^+$ T lymphocytes belonged to $CD4^+$ as well as $CD8^+$ T lymphocytes (Table 2). In line with what was observed in the first experiment, and in striking contrast to the other tested D_{752} isolates, the most important carrier cells for the neurovirulent isolate 03P37 were $CD172a^+$ cells, followed by a smaller portion of infected T lymphocytes (Table 2). Although no differences were observed in infected cell type between D_{752} and N_{752} isolates, with the exception of 03P37, a clear difference was observed in the number of single EHV-1-infected cells in the lamina propria between

(a)

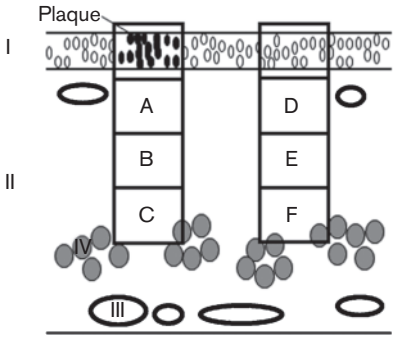

(b)

Isolate	Tissue	ROI	Time p.i. (h)					
			0	12	24	36	48	72
97P70	Septum	A	0±0	0±0	0±0	36±8	157±44	233±51
		B	0±0	0±0	0±0	21±5	102±17	133±17
		C	0±0	0±0	0±0	0±0	19±4	51±12
		D	0±0	0±0	0±0	6±3	20±6	37±11
		E	0±0	0±0	0±0	4±2	19±2	28±4
		F	0±0	0±0	0±0	0±0	9±1	21±7
	Nasopharynx	A	0±0	0±0	0±0	9±5	139±22	307±58
		B	0±0	0±0	0±0	3±1	77±17	112±24
		C	0±0	0±0	0±0	0±0	33±5	53±14
		D	0±0	0±0	0±0	1±1	19±5	31±6
		E	0±0	0±0	0±0	0±0	14±2	26±3
		F	0±0	0±0	0±0	0±0	6±1	16±4
03P37	Septum	A	0±0	0±0	16±10	108±37	165±31	268±44
		B	0±0	0±0	12±3	26±11	111±20	207±16
		C	0±0	0±0	4±1	3±2	54±15	126±21
		D	0±0	0±0	5±1	8±6	25±8	75±18
		E	0±0	0±0	4±2	3±1	23±7	41±12
		F	0±0	0±0	0±0	1±0	14±7	36±8
	Nasopharynx	A	0±0	0±0	29±8	19±4	152±23	246±37
		B	0±0	0±0	25±9	16±5	118±17	152±36
		C	0±0	0±0	21±5	12±2	20±4	66±20
		D	0±0	0±0	5±1	9±3	19±5	27±5
		E	0±0	0±0	8±3	7±2	17±1	20±8
		F	0±0	0±0	4±1	3±1	8±3	23±3

Fig. 2. Quantification of single EHV-1-infected cells in different zones of nasal septum and nasopharynx for a non-neurovirulent (97P70) and a neurovirulent (03P37) EHV-1 strain. (a) Schematic overview of the structure of the nasal septum and nasopharynx with the different analysed regions of interest as described in Methods. I, Epithelium; II, connective tissue; III, blood vessel; IV, glands. (b) One hundred sections of the tissues were made per time point and the total number of infected cells per zone and per time point were determined. The data shown represent means ± SD of triplicate independent experiments. ROI, Region of interest.

the isolates. It was apparent that neurovirulent D_{752} isolates had a greater number of EHV-1-infected cells in the lamina propria compared with N_{752} isolates (Fig. 4). Although these results were similar to what was observed in the first experiment, they did not reach significance due to variation between the N_{752} isolates.

Based on this second experiment including more Belgian D_{752} and N_{752} isolates, we concluded that, for the N_{752} isolates a higher number of epithelial plaques could be found, and for the D_{752} isolates there was a faster migration through the BM barrier via single EHV-1-infected cells along with a greater number of single EHV-1-infected cells below the BM barrier.

The SNP in the EHV-1 polymerase is not responsible for the observed differences in epithelial plaque number and immune cell tropism, but is important for invasion kinetics as well as infection rate of immune cells

Finally, a third experiment was performed to test the hypothesis that the D/N SNP in the ORF30 polymerase and

Table 1. Percentage of marker-positive EHV-1-infected individual cells at various time points after inoculation with two Belgian EHV-1 isolates

Time (h p.i.)	Percentage of marker-positive EHV-1-infected individual cells in 20 cryosections per cell marker									
	97P70					03P37				
	CD172a$^+$	CD5$^+$	CD4$^+$	CD8$^+$	IgM$^+$	CD172a$^+$	CD5$^+$	CD4$^+$	CD8$^+$	IgM$^+$
24	0.0±0.0	0.0±0.0	0.0±0.0	0.0±0.0	0.0±0.0	74.1±7.3	12.5±4.4	14.3±7.4	4.9±1.6	0.0±0.0
36	38.6±21.6	19.7±19.5	37.3±17.2	4.3±3.5	0.0±0.0	70.9±20.0	18.1±16.3	22.8±11.2	12.4±2.4	0.7±1.2
48	26.2±1.3	47.2±11.4	40.5±19.3	24.7±4.8	2.9±1.4	69.4±6.0	11.0±2.0	13.9±3.5	6.4±3.6	0.8±0.3
72	30.4±9.8	53.9±5.9	50.0±21.9	25.1±7.2	1.9±1.3	73.4±12.9	14.3±1.2	13.7±6.3	7.7±3.4	0.9±0.6

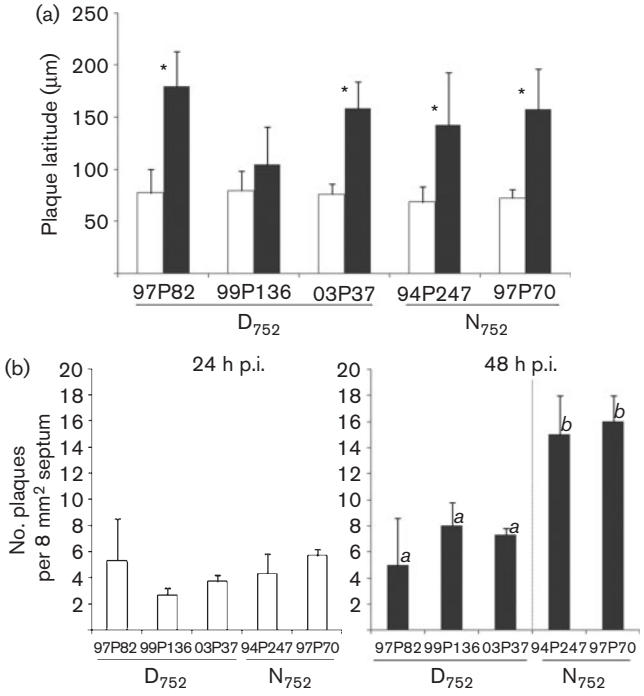

Fig. 3. Evolution of plaque formation in epithelium of nasal explants for various Belgian neurovirulent and non-neurovirulent EHV-1 isolates. Equine respiratory mucosal explants were inoculated with several Belgian neurovirulent (D_{752}) or non-neurovirulent (N_{752}) isolates. At 0, 24 and 48 h p.i., explants were collected, and 100 consecutive sections were made and analysed to determine plaque latitude (a) and the number of plaques (b). Empty bars, 24 h p.i.; filled bars, 48 h p.i. All data represent means+SD of triplicate independent experiments. Asterisks indicate statistically significant differences ($P \leqslant 0.05$). Data with a different letter (*a* or *b*) are significantly different from one another.

the observed differences between the Belgian D_{752} and N_{752} isolates are linked. To this end, explants from the same horse were inoculated with the non-neurovirulent (N_{752}) NY03 or neurovirulent (D_{752}) Ab4 reference strain or their respective D/N recombinant viruses. These viruses are completely identical in their genomic background with the exception of the SNP at position 752 in the ORF30 DNA polymerase.

At both 24 and 48 h p.i., no differences were observed in plaque latitudes between the D_{752} and N_{752} revertant viruses, but in line with our previous experiments, a significant increase in plaque latitude was observed between these two time points p.i. (data not shown). The differences in plaque numbers at 48 h p.i., as seen previously between the D_{752} and N_{752} Belgian isolates (Fig. 3), could not be confirmed using the D/N revertant viruses. No significant differences in the number of plaques at 48 h p.i. were observed between the D/N recombinant viruses of either Ab4 (neurovirulent in origin) or NY03 (non-neurovirulent in origin) (Fig. 5a). This indicated that the differences in plaque numbers could not be attributed to the D/N SNP.

Despite this, a role for the D/N SNP in invasion kinetics and number of infected immune cells could be observed. For parental Ab4, the D_{752} revertant Ab4 and the D_{752} mutant NY03 virus strains, all typed as neurovirulent, single EHV-1-infected cells were present at 24 h p.i. below the BM, whereas for the parental NY03, the N_{752} revertant NY03 and the N_{752} Ab4 mutant, infected cells were only present starting from 48 h p.i. (Table 3). Interestingly, the strains with D_{752} in the ORF30 region (D_{752} revertant Ab4 and D_{752} mutant NY03) showed a significantly greater number of individual EHV-1-infected cells below the BM when compared with the N_{752} strains (Fig. 5b).

A difference in leukocyte tropism between 03P37 (D_{752}) and 97P70 (N_{752}), two Belgian field isolates, was observed, but this difference was not apparent using other Belgian D and N field isolates (Table 2). Therefore, the leukocyte tropism of Ab4, NY03 and their D/N recombinant viruses was evaluated to determine whether the D/N SNP in the catalytic subunit of the viral DNA polymerase could be responsible for the exceptional behaviour of 03P37 or not. Using the Ab4 and NY03 recombinant viruses, no difference in leukocyte tropism was observed and individual infected cells were equally identified as $CD5^+$ T

Table 2. Percentage of marker-positive EHV-1-infected individual cells for different Belgian EHV-1 isolates

SNP/isolate	Percentage of marker-positive EHV-1-infected individual cells in 20 cryosections per cell marker									
	24 h p.i.					48 h p.i.				
	$CD172a^+$	$CD5^+$	$CD4^+$	$CD8^+$	IgM^+	$CD172a^+$	$CD5^+$	$CD4^+$	$CD8^+$	IgM^+
D_{752}										
97P82	86.1±2.4	4.2±7.2	0.0±0.0	0.0±0.0	0.0±0.0	45±1.6	44.8±5.1	31.1±3	15.2±3.2	2.4±1.7
99P136	81.1±20	0.0±0.0	0.0±0.0	0.0±0.0	0.0±0.0	39.9±2.4	51.1±4.1	35.4±19.7	16±9.5	0.0±0.0
03P37	83±2.9	9.9±4.4	0.0±0.0	0.0±0.0	0.0±0.0	65.5±7.4	23.1±7.5	13.1±4.2	11±2.3	1.8±1.8
N_{752}										
94P247	0.0±0.0	0.0±0.0	0.0±0.0	0.0±0.0	0.0±0.0	26.8±4	39.9±1.9	25.8±17.8	17.9±10.5	3.4±0.9
97P70	0.0±0.0	0.0±0.0	0.0±0.0	0.0±0.0	0.0±0.0	25.8±1.3	50.7±14	43±7.3	28±6.1	0.0±0.0

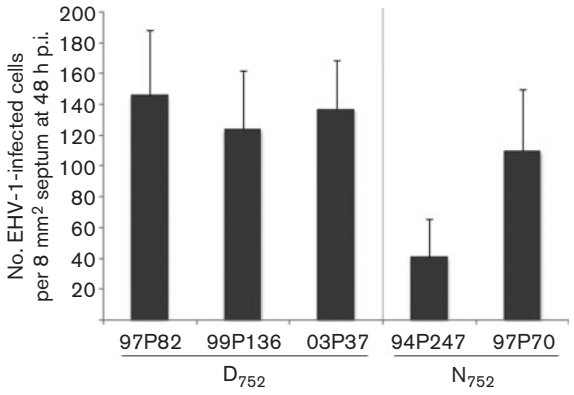

Fig. 4. Total number of single EHV-1-infected cells for different EHV-1 isolates in equine nasal explants. For each isolate tested, every tenth section of a serially sectioned block of tissue was collected and 100 sections were counted in total. Data shown represent means + SD of triplicate independent experiments.

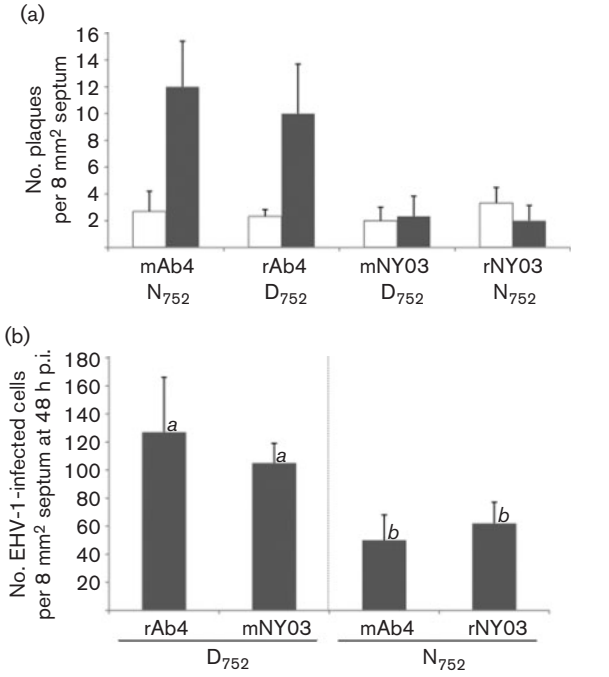

Fig. 5. Replication characteristics of strains Ab4 and NY03 and their recombinant viruses. Equine respiratory mucosal explants were inoculated with the N_{752}/D_{752} recombinant viruses of strains Ab4 (reference neurovirulent strain) and NY03 (reference non-neurovirulent strain). At 0, 24 and 48 h p.i., explants were collected and analysed. Empty bars, 24 h p.i.; filled bars, 48 h p.i. Data shown represent means + SD of triplicate independent experiments. Data carrying a different letter (*a* or *b*) are significantly different from one another. m, Recombinant mutant virus; r, recombinant revertant virus. (a) Number of plaques in epithelium of nasal explants in 100 consecutive sections. (b) Total amount of individual EHV-1-infected cells counted below the BM for every strain at 48 h p.i. Every tenth section of a serially sectioned block of tissue was collected and 100 sections were counted in total.

lymphocytes and $CD172a^+$ cells at 48 h p.i. (Table 3). In addition, the infected T lymphocytes consisted of $CD4^+$ and to a lesser extent $CD8^+$ T lymphocytes (Table 3).

With this final experiment, we could show that the D/N SNP was not responsible for differences in plaque number or for the tropism of immune cells. However, the D/N SNP appeared to be responsible for (i) faster invasion kinetics of D_{752} strains compared with N_{752} strains, and (ii) higher infection rates of infected cells below the BM barrier when EHV-1 carried the D_{752} genotype.

DISCUSSION

In general, respiratory alphaherpesviruses start their pathogenesis in the upper respiratory tract where primary replication occurs in epithelial cells and results in upper respiratory tract disease. Hereafter, they invade through the BM and the underlying lamina propria, where the virus can reach blood vessels and rapidly disseminate in the body via a cell-associated viraemia. This enables the virus to reach secondary target organs where replication can cause severe symptoms such as abortion and nervous system disorders (Sabo *et al.*, 1969; Wyler *et al.*, 1989; Gibson *et al.*, 1992). Recently, Glorieux *et al.* (2007) studied the replication and invasion strategies of pseudorabies virus (PRV; suid herpesvirus 1), a porcine alphaherpesvirus, in porcine nasal mucosal explants. With this novel *in vitro* system, it was seen that PRV spread horizontally as well as vertically in a plaque-wise manner in the epithelium, and that PRV-induced plaques penetrated the BM barrier between 12 and 24 h p.i. (Glorieux *et al.*, 2007). Importantly, these observations were consistent with previous *in vivo* observations of PRV replication (Pol *et al.*, 1989). In the present study, we studied the replication and invasion strategies of EHV-1, a respiratory alphaherpesvirus in horses of paramount economic importance, in a recently established equine respiratory mucosa explant model (Vandekerckhove *et al.*, 2009). Briefly, EHV-1-induced plaques were present in the epithelium starting from 24 h p.i. and showed an increase in plaque latitude over time. In striking contrast to what was observed for PRV, the spread of EHV-1-induced plaques was solely lateral. This lateral spread in the epithelium was clearly more pronounced for some EHV-1 isolates, but no correlation was found with the recently identified SNP in the DNA polymerase of the virus associated with neurovirulent potential (Nugent *et al.*, 2006). In addition, by using the different recombinant viruses Ab4 and NY03 harbouring the single D/N point mutation, we observed that there was a difference in number of plaques between these two viruses independent of the D/N variant, which indicates that other virus characteristics beyond ORF30 are important for virus replication in the upper respiratory tract. This is in line with what has been observed in many other studies (Lunn

Table 3. Percentage of marker-positive EHV-1-infected individual cells for different EHV-1 strains and their recombinant viruses

Rev, Revertant; Mut, strain with the ORF30 mutation.

SNP/isolate	Percentage of marker-positive EHV-1-infected individual cells in 20 cryosections per cell marker									
	24 h p.i.					48 h p.i.				
	CD172a$^+$	CD5$^+$	CD4$^+$	CD8$^+$	IgM$^+$	CD172a$^+$	CD5$^+$	CD4$^+$	CD8$^+$	IgM$^+$
D_{752}										
Ab4	84.4±3.9	15.6±3.9	0.0±0.0	10.8±10.4	0.0±0.0	29±0.9	39.9±1.3	35.3±9.1	18.1±11	0.0±0.0
Rev Ab4	79.3±6.9	4.8±8.3	0.0±0.0	0.0±0.0	0.0±0.0	35.5±19.8	31.9±13.8	37.1±11.1	37.6±14.6	0.3±0.3
Mut NY03	76.7±25.2	0.0±0.0	0.0±0.0	0.0±0.0	0.0±0.0	34.7±7.3	30.8±1.8	30.8±7.7	16.1±2.9	0.8±0.3
N_{752}										
NY03	0.0±0.0	0.0±0.0	0.0±0.0	0.0±0.0	0.0±0.0	25.3±6	34.9±2.2	31.8±8.7	20.4±1.8	1.7±0.6
Rev NY03	0.0±0.0	0.0±0.0	0.0±0.0	0.0±0.0	0.0±0.0	33.5±1.9	36.3±5.9	30.5±7.6	17.2±4.9	2.2±1.4
Mut Ab4	0.0±0.0	0.0±0.0	0.0±0.0	0.0±0.0	0.0±0.0	37.6±11.3	35±15.3	34±3.6	22.7±6.5	0.0±0.0

et al., 2009). As plaques never crossed the BM at any time point p.i., this implies that the BM functions as an absolute barrier. Remarkably, however, single EHV-1-infected cells were observed below the BM in the vicinity of virus-induced plaques, although destruction of the BM by EHV-1-induced plaques was never observed. Hence, these results suggest that closely related alphaherpesviruses can use very different ways of crossing the BM barrier and invading the respiratory mucosa. Whereas it was previously shown that the alphaherpesvirus PRV crosses the BM in an aggressive, plaque-wise manner (Glorieux *et al.*, 2007), we showed in the present study that EHV-1 penetrates the deeper tissues of the respiratory tract in a more discrete manner, using migrating individual cells as Trojan horses.

When evaluating the invasion mechanisms of different EHV-1 isolates more thoroughly, differences were observed depending on the EHV-1 isolate used. An important finding was the absence of single EHV-1-infected cells below the BM barrier at 24 h p.i. for all non-neurovirulent EHV-1 isolates carrying the N_{752} genotype in their DNA polymerase when compared with neurovirulent, D_{752} isolates. What the underlying mechanism is for this faster breakthrough through the BM barrier of neurovirulent isolates remains to be elucidated, but we can state that (i) the D/N_{752} SNP is important for this phenomenon and (ii) the time-dependent difference in spread through the BM is not an artefact in our system, as similar observations have been made *in vivo* (Gryspeerdt *et al.*, 2010). Indeed, single EHV-1-infected cells below the BM were seen starting from 1 day p.i. for 03P37, a neurovirulent D_{752} isolate, whereas for the non-neurovirulent N_{752} isolate 97P70, single infected cells were observed as early as 2 days p.i. in this *in vivo* experiment (Gryspeerdt *et al.*, 2010). In our nasal explant system, we observed no differences in cell tropism between D_{752} and N_{752} isolates, and EHV-1-infected cells were equally identified as CD5$^+$ T lymphocytes and CD172a$^+$ CML. One Belgian isolate used in this study, the neurovirulent 03P37, was a clear exception with significantly more infected CML than CD5$^+$ T lymphocytes. As 03P37 was the most recently isolated strain used in this study (2003), a possible explanation for this observation could be that the leukocyte tropism of circulating EHV-1 isolates changes over time. To evaluate this hypothesis, we studied the replication kinetics of recent Belgian D_{752} and N_{752} isolates from 2009. For these recent EHV-1 isolates, CML and CD5$^+$ T lymphocytes were equally infected, indicating that the leukocyte tropism had not changed over time (data not shown). These results do not indicate that recent EHV-1 strains evolve to another leukocyte tropism and, as a result, we have as yet no explanation for the unusual leukocyte tropism of the Belgian isolate 03P37. Another interesting finding was a twofold higher infection of CD4$^+$ T lymphocytes compared with CD8$^+$ T lymphocytes for all EHV-1 isolates examined in the present study. CD4$^+$ and CD8$^+$ T lymphocytes are both crucial for the establishment of an efficient cellular immune response. CD4$^+$ T lymphocytes assist other leukocytes in processes such as maturation of B cells and activation of CD8$^+$ T lymphocytes and macrophages. In association with MHC class I molecules, CD8$^+$ T lymphocytes recognize and destroy virus-infected cells. Cellular immunity is most important in controlling an EHV-1 infection as neutralizing antibodies have been shown not to be fully protective (Kydd *et al.*, 2006). Many factors indicate that T lymphocytes play an important role in the clearance of EHV-1 from the horse: (i) EHV-1 becomes intracellular within hours p.i. and (ii) CD8$^+$ T lymphocytes increase in the blood and lungs after infection (Kydd *et al.*, 2006). Therefore, it is not surprising that EHV-1 preferentially infects T lymphocytes, as this could allow the virus to persist in its host for a longer period of time before being eliminated.

In general, our findings in the equine nasal mucosal explant system indicated that N_{752} strains are more prone to replicate in epithelial cells, whilst D_{752} strains are superior at infecting immune cells. This was shown by the greater number of plaques in the epithelium upon infection with N_{752} strains and their slower invasion kinetics to the

connective tissue below the BM via infected immune cells. D_{752} strains, in contrast, had a lower number of epithelial plaques, but crossed the BM barrier earlier and with a significantly greater number of infected immune cells. Indeed, we observed that isolates with the D_{752} genotype had significantly more single EHV-1-infected cells below the BM than isolates with the N_{752} genotype, at 48 h p.i. This is in agreement with several other studies, showing a more robust replication of neurovirulent D_{752} isolates, as shown by a higher level of viraemia of infected cells in the blood (Allen & Breathnach, 2006; Goodman *et al.*, 2006, 2007; Allen, 2008; Van de Walle *et al.*, 2009).

To date, the mouse model is used as a valid *in vivo* model for studying virological and histological aspects of EHV-1-induced disease in the horse (Walker *et al.*, 1999). A big concern, however, is the heterologous nature of this animal model, which can make it difficult to make valid comparisons and extrapolations to the natural host of the virus, the horse (Walker *et al.*, 1999). Our *in vitro* model is a good representation of the *in vivo* situation in the natural host, as the results obtained in our study were virtually identical to those obtained in a recent *in vivo* pathogenesis study in horses by Gryspeerdt *et al.* (2010). Moreover, differences in invasion kinetics and infection rates between neurovirulent and non-neurovirulent EHV-1 isolates were identified, indicating that our *in vitro* respiratory mucosal explant system is a valuable alternative to provide novel information in addition to the currently existing EHV-1 models.

In conclusion, the equine respiratory explant system can be used for studying the early pathogenesis of EHV-1 strains and deletion mutants with known neurovirulence, for testing the potential of various vaccines and for investigating the efficacy of antiviral drugs on EHV-1 infection at the primary site of replication, the upper respiratory tract.

METHODS

Donor horses. Material from slaughter horses was used to obtain nasal explants. All horses were between 4 and 7 years old, based on inspection of the dental incisive architecture (Muylle *et al.*, 1996), and were inspected for nasal/ocular discharge and lung pathology. A complement-dependent seroneutralization test was performed on the serum of all horses and EHV-specific antibody titres ranged between 4 and 64.

Cultivation of nasal explants. The cultivation of nasal explants was performed exactly as described previously (Vandekerckhove *et al.*, 2009). In brief, immediately after slaughter, the head was removed from the carcass and sawn longitudinally into two equal sections. Tissue from the deep intranasal part of the septum and the nasopharynx was collected. The tissue was transported on ice in PBS, supplemented with 1 μg gentamicin (Gibco) ml^{-1}, 1 mg streptomycin (Certa) ml^{-1}, 1000 U penicillin (Continental Pharma) ml^{-1}, 1 mg kanamycin (Sigma) ml^{-1} and 5 μg Fungizone ml^{-1}, to the laboratory. Mucosal explants were stripped from the surface of the different tissues by use of surgical blades (Swann-Morton). The stripped mucosa of each tissue was divided into equal explants of 25 mm^2 and placed epithelium upwards on fine-meshed gauze for culture at the air–liquid interface. Only a thin film of serum-free medium [50 % RPMI/50 % Dulbecco's modified Eagle's medium; Gibco) supplemented with 0.3 mg glutamine (BHD Biochemical) ml^{-1}, 1 μg gentamicin ml^{-1}, 0.1 mg streptomycin ml^{-1} and 100 U penicillin ml^{-1}] covered the explants, thereby mimicking the air–liquid interface found in the respiratory tract of the living animal. Explants were maintained at 37 °C in an atmosphere containing 5 % CO_2.

Viruses. Different Belgian EHV-1 strains were included in this study and were genotyped in the ORF30 region by the Animal Health Trust, UK (Nugent *et al.*, 2006). The isolates 94P247 and 97P70 were isolated from the lungs of aborted fetuses in 1994 and 1997, respectively, and typed as non-neurovirulent. The isolates 97P82, 99P136 and 03P37 were isolated from the peripheral blood mononuclear cells of paralytic horses in 1997, 1999 and 2003, respectively, and typed as neurovirulent. Parental Ab4 (reference neurovirulent strain, containing D_{752} in ORF30), N_{752} mutant (D_{752}→N mutation) and D_{752} revertant (N_{752}→D substitution) recombinant viruses, and parental NY03 (reference non-neurovirulent strain, containing N_{752}), D_{752} mutant (N_{752}→D mutation) and N_{752} revertant (D_{752}→N substitution) recombinant viruses, were also included in this study (Goodman *et al.*, 2007; Van de Walle *et al.*, 2009).

All virus stocks used for inoculation were at the sixth passage, after two passages in rabbit kidney (RK13) cells and four subsequent passages in equine embryonic lung cells. In addition, all virus stocks used for inoculation were sequenced in their ORF30 region to confirm the correct genotype (data not shown).

Inoculation of nasal explants. All explants were inoculated after 24 h culture. Inoculation took place by immersion of the explant in 1 ml inoculum, containing $10^{6.5}$ 50 % tissue culture infectious doses of EHV-1 for 1 h at 37 °C and 5 % CO_2. After incubation, the explants were washed twice with warm medium and transferred back to their gauze. At several time points p.i., explants were collected, embedded in methylcellulose medium (Methocel MC; Sigma-Aldrich) and frozen at −70 °C.

In the first experiment, six individual slaughter horses were divided into two groups. Nasal and nasopharyngeal explants of the three individual horses from the first group were inoculated with the D_{752} isolate 03P37, whilst nasal and nasopharyngeal explants of the other three horses were inoculated with the N_{752} isolate 97P70. For each animal, one explant was examined at each collected time point (0, 12, 24, 36, 48 and 72 h p.i.).

In the second and third experiment, the nasal explants of three horses were collected. For each horse, several explants were made and inoculated with different EHV-1 isolates (94P247, 97P70, 97P82, 99P136, 03P37, parental Ab4, mutant Ab4, revertant Ab4, parental NY03, mutant NY03 and revertant NY03) and collected at different time points (0, 24 and 48 h p.i.).

Plaque analysis and penetration of virus plaques through the BM. At 0, 12, 24, 36, 48 and 72 h p.i., 100 consecutive cryosections of 16 μm were made from the frozen explants and the cryosections were fixed in 100 % methanol for 20 min at −20 °C. Subsequently, the BM of the tissues was stained with monoclonal mouse anti-collagen VII antibodies (Sigma-Aldrich), followed by secondary Texas red-labelled goat anti-mouse antibodies (Molecular Probes). In a second step, viral proteins were stained by incubation with biotinylated equine polyclonal anti-EHV-1 IgG (van der Meulen *et al.*, 2003), followed by streptavidin–fluorescein isothiocyanate (FITC; Molecular Probes). Antibodies were incubated for 1 h at 37 °C and 5 % CO_2. Finally, the cryosections were washed three times in PBS and mounted with glycerine/1,4-diazabicyclo[2.2.2]octane (DABCO; Janssen Chimica). All stainings were analysed with a confocal laser-scanning microscope (TCS SP2 Laser Scanning Spectral Confocal System; Leica Microsystems) using Leica confocal software. To analyse the replication characteristics of several EHV-1

isolates reproducibly, we used a system set up by Glorieux *et al.* (2009). Briefly, penetration of the virus through the BM was inspected and virus plaque latitudes and plaque volumes were measured in 100 consecutive cryosections using the freely available ImageJ version 1.28 software (http://rsb.info.nih.gov/ij/docs/intro.html). For each cryosection, a stack of *z*-series was made. A *z*-series was defined as a series of images in the axis perpendicular to the image plane, so in the depth of the tissue. Hereafter, voxels (defined as a volume element that represents a value in three-dimensional space) positive for FITC fluorescence were counted. To cover an entire plaque, different cryosections were combined. Finally, the total number of voxels was multiplied by voxel volume to obtain plaque volume. Plaque latitude was measured by means of the line tool in ImageJ.

Quantification and characterization of individual infected cells. Immunofluorescent double stainings were used to quantify and characterize individual infected cells below the BM. At different time points p.i., 100 cryosections of 16 μm were made and fixed in 100 % methanol for 20 min at −20 °C. Every tenth section of a serially sectioned block of tissue was collected. Twenty cryosections were stained for each cell-surface marker separately. In the first step, the monoclonal antibodies HT23A, HB61A, 73/6.9.1, DH59B and 1.9/3.2 (VMRD) were used as markers for $CD5^+$ T lymphocytes (pan-equine T-lymphocyte marker), $CD4^+$ T lymphocytes (helper T lymphocytes), $CD8^+$ T lymphocytes (cytotoxic T lymphocytes), $CD172a^+$ cells from the monocyte lineage (CML) or B lymphocytes (IgM^+), respectively. As controls, (i) stainings were performed on uninfected tissue and (ii) corresponding isotype control antibodies were included. Subsequently, cryosections were incubated with secondary Texas red-labelled goat anti-mouse antibodies. In the second step, all cryosections were stained for viral proteins by incubation of biotinylated equine polyclonal anti-EHV-1 IgG (van der Meulen *et al.*, 2003), followed by streptavidin–FITC. In general, antibodies were incubated for 1 h at 37 °C and 5 % CO_2. Finally, cryosections were washed three times in PBS and mounted with glycerine/DABCO. The number of individual infected cells below the BM, as well as their identity, was determined by confocal laser-scanning microscopy. Therefore, two defined regions of interest were taken into account in the cryosections: one region with a plaque situated in the epithelium and one region without a plaque in the epithelium (Fig. 2a). These regions were subsequently subdivided into three further regions: A, B and C for the regions below a plaque and D, E and F for the regions without a plaque.

Statistical analysis. Data were analysed by a mixed model with the horse as the random effect and strain, time and their interaction as categorical effects (SAS version 9.2; SAS Corp.). *F*-tests were performed at the 5 % global significance level. *P* values for pairwise comparisons between the strains were adjusted for multiple comparisons using Tukey's method. The data were presented as means ± SD.

ACKNOWLEDGEMENTS

This research was supported by the Institute for the Promotion of Innovation through Science and Technology in Flanders (IWT-Vlaanderen). We thank Carine Boone, Chris Bracke and Chantal Vanmaercke for their excellent technical assistance. We thank Jan Van Doorsselaere for the sequencing experiment.

REFERENCES

Allen, G. P. (2008). Risk factors for development of neurologic disease after experimental exposure to equine herpesvirus-1 in horses. *Am J Vet Res* **69**, 1595–1600.

Allen, G. P. & Breathnach, C. C. (2006). Quantification by real-time PCR of the magnitude and duration of leucocyte-associated viraemia in horses infected with neuropathogenic vs. non-neuropathogenic strains of EHV-1. *Equine Vet J* **38**, 252–257.

Allen, G. P. & Bryans, J. T. (1986). Molecular epizootiology, pathogenesis, and prophylaxis of equine herpesvirus-1 infections. *Prog Vet Microbiol Immunol* **2**, 78–144.

Awan, A. R., Chong, Y.-C. & Field, H. J. (1990). The pathogenesis of equine herpesvirus type 1 in the mouse: a new model for studying host responses to the infection. *J Gen Virol* **71**, 1131–1140.

Brosnahan, M. M. & Osterrieder, N. (2009). Equine herpesvirus-1: a review and update. In *Infectious Diseases of the Horse*, pp. 41–51. Edited by T. S. Mair & R. E. Hutchinson. Fordham: Equine Veterinary Journal.

Bryans, J. T. & Allen, G. P. (1989). Herpesviral diseases of the horse. In *Herpesviral Diseases of Cattle, Horses and Pigs*, pp. 176–229. Edited by G. Wittman. Boston: Kluwer.

Galosi, C. M., Barbeito, C. G., Vila Rosa, M. V., Cid de la Paz, V., Ayala, M. A., Corva, S. G., Etcheverrigaray, M. E. & Gimeno, E. J. (2004). Argentine strain of equine herpesvirus 1 isolated from an aborted foetus shows low virulence in mouse respiratory and abortion models. *Vet Microbiol* **103**, 1–12.

Gibson, J. S., Slater, J. D., Awan, A. R. & Field, H. J. (1992). Pathogenesis of equine herpesvirus-1 in specific pathogen-free foals: primary and secondary infections and reactivation. *Arch Virol* **123**, 351–366.

Glorieux, S., Van den Broeck, W., van der Meulen, K. M., van Reeth, K., Favoreel, H. W. & Nauwynck, H. J. (2007). *In vitro* culture of porcine respiratory nasal mucosa explants for studying the interaction of porcine viruses with the respiratory tract. *J Virol Methods* **142**, 105–112.

Glorieux, S., Favoreel, H. W., Meesen, G., de Vos, W., Van den Broeck, W. & Nauwynck, H. J. (2009). Different replication characteristics of historical pseudorabies virus strains in porcine respiratory nasal mucosa explants. *Vet Microbiol* **136**, 341–346.

Goodman, L. B., Wagner, B., Flaminio, M. J., Sussman, K. H., Metzger, S. M., Holland, R. & Osterrieder, N. (2006). Comparison of the efficacy of inactivated combination and modified-live virus vaccines against challenge infection with neuropathogenic equine herpesvirus type 1 (EHV-1). *Vaccine* **24**, 3636–3645.

Goodman, L. B., Loregian, A., Perkins, G. A., Nugent, J., Buckles, E. L., Mercorelli, B., Kydd, J. H., Palù, G., Smith, K. C. & other authors (2007). A point mutation in a herpesvirus polymerase determines neuropathogenicity. *PLoS Pathog* **3**, e160.

Gryspeerdt, A., Vandekerckhove, A. P., Garré, B., Barbé, F., Van de Walle, G. R. & Nauwynck, H. J. (2010). Differences in replication kinetics and cell tropism between neurovirulent and non-neurovirulent EHV1 strains during the acute phase of infection in horses. *Vet Microbiol* **142**, 242–253.

Kohn, C. W., Reed, S. M., Sofaly, C. D., Henninger, R. W., Saville, W. J., Allen, G. P. & Premanadan, C. (2006). Transmission of EHV-1 in horses with EHV-1 myeloencephalopathy: implications for biosecurity and review. *Clin Tech Equine Pract* **5**, 60–66.

Kydd, J. H., Smith, K. C., Hannant, D., Livesay, G. J. & Mumford, J. A. (1994a). Distribution of equid herpesvirus-1 (EHV-1) in the respiratory tract associated lymphoid tissue: implications for cellular immunity. *Equine Vet J* **26**, 470–473.

Kydd, J. H., Smith, K. C., Hannant, D., Livesay, G. J. & Mumford, J. A. (1994b). Distribution of equid herpesvirus-1 (EHV-1) in the respiratory tract of ponies: implications for vaccination strategies. *Equine Vet J* **26**, 466–469.

Kydd, J. H., Townsend, H. G. & Hannant, D. (2006). The equine immune response to equine herpesvirus-1: the virus and its vaccines. *Vet Immunol Immunopathol* **111**, 15–30.

Lunn, D. P., Davis-Poynter, N., Flaminio, M. J., Horohov, D. W., Osterrieder, K., Pusterla, N. & Townsend, H. G. (2009). Equine herpesvirus-1 consensus statement. *J Vet Intern Med* **23**, 450–461.

Muylle, S., Simoens, P. & Lauwers, H. (1996). Ageing horses by an examination of their incisor teeth: an (im)possible task? *Vet Rec* **138**, 295–301.

Nugent, J., Birch-Machin, I., Smith, K. C., Mumford, J. A., Swann, Z., Newton, J. R., Bowden, R. J., Allen, G. P. & Davis-Poynter, N. (2006). Analysis of equid herpesvirus 1 strain variation reveals a point mutation of the DNA polymerase strongly associated with neurovirulent versus nonneurovirulent disease outbreaks. *J Virol* **80**, 4047–4060.

Patel, J. R. & Heldens, J. (2005). Equine herpesviruses 1 (EHV-1) and 4 (EHV-4) – epidemiology, disease and immunoprophylaxis: a brief review. *Vet J* **170**, 14–23.

Perkins, G. A., Goodman, L. B., Tsujimura, K., Van de Walle, G. R., Kim, S. G., Dubovi, E. J. & Osterrieder, N. (2009). Investigation of the prevalence of neurologic equine herpes virus type 1 (EHV-1) in a 23-year retrospective analysis (1984–2007). *Vet Microbiol* **139**, 375–378.

Pol, J. M. A., Gielkens, A. L. J. & Van Oirschot, J. T. (1989). Comparative pathogenesis of three strains of pseudorabies virus in pigs. *Microb Pathog* **7**, 361–371.

Pusterla, N., Wilson, W. D., Madigan, J. E. & Ferraro, G. L. (2009). Equine herpesvirus-1 myeloencephalopathy: a review of recent developments. *Vet J* **180**, 279–289.

Sabo, A., Rajcani, J. & Blaskovic, D. (1969). Studies on the pathogenesis of Aujeszky's disease. III. The distribution of virulent virus in piglets after intranasal infection. *Acta Virol* **13**, 407–414.

Timoney, J. F. (2004). The pathogenic equine streptococci. *Vet Res* **35**, 397–409.

USDA APHIS (2007). Equine herpesvirus myeloencephalopathy: a potentially emerging disease. Available at: http://www.aphis.usda.gov/animal_health/emergingissues/downloads/ehv1final.pdf. Accessed 9 December 2008. US Department of Agriculture Animal and Plant Health Inspection Service.

Vandekerckhove, A., Glorieux, S., Van den Broeck, W., Gryspeerdt, A., van der Meulen, K. M. & Nauwynck, H. J. (2009). *In vitro* culture of equine respiratory mucosa explants. *Vet J* **181**, 280–287.

van der Meulen, K. M., Vercauteren, G., Nauwynck, H. J. & Pensaert, M. B. (2003). A local epidemic of equine herpesvirus 1-induced neurological disorders in Belgium. *Flem Vet J* **72**, 366–372.

Van de Walle, G. R., Goupil, R., Wishon, C., Damiani, A., Perkins, G. A. & Osterrieder, N. (2009). A single-nucleotide polymorphism in a herpesvirus DNA polymerase is sufficient to cause lethal neurological disease. *J Infect Dis* **200**, 20–25.

Van Maanen, C. (2002). Equine herpesvirus 1 and 4 infections: an update. *Vet Q* **24**, 58–78.

Van Maanen, C. & Cullinane, A. (2002). Equine influenza virus infections: an update. *Vet Q* **24**, 79–94.

Van Woensel, P. A. M., Goovaerts, D., Markx, D. & Visser, N. (1995). A mouse model for testing the pathogenicity of equine herpes virus-1 strains. *J Virol Methods* **54**, 39–49.

Walker, C., Love, D. N. & Whalley, J. M. (1999). Comparison of the pathogenesis of acute equine herpesvirus 1 (EHV-1) infection in the horse and the mouse model: a review. *Vet Microbiol* **68**, 3–13.

Wyler, R., Engels, M. & Schwyzer, M. (1989). Infectious bovine rhinotracheitis/vulvovaginitis (BHV1). In *Herpesvirus Diseases of Cattle, Horses, and Pigs*, pp. 1–72. Edited by G. Wittman. Dordrecht: Kluwer Academic Publishers.

Yamada, S., Matsumara, T., Tsjujimura, K., Yamaguchi, T., Ohya, K. & Fukushi, H. (2008). Comparison of the growth kinetics of neurovirulent and nonneurovirulent equid herpesvirus type 1 (EHV-1) strains in cultured murine neuronal cells and the relevance of the D/N_{752} coding change in DNA polymerase gene (ORF30). *J Vet Med Sci* **70**, 505–511.